

Understanding the cross section of $e^+e^- \rightarrow \eta J/\psi$ process via nonrelativistic QCD

Cong-Feng Qiao*

*School of Physics, University of Chinese Academy of Sciences
YuQuan Road 19A, Beijing 100049, China and
Collaborative Innovation Center for Particles and Interaction, USTC, HeFei 230026, China*

Rui-Lin Zhu†

*School of Physics, University of Chinese Academy of Sciences
YuQuan Road 19A, Beijing 100049, China and
Nuclear Science Division, Lawrence Berkeley National Lab, Berkeley, CA 94720, USA*

Motivated by the large cross section of $e^+e^- \rightarrow \eta J/\psi$ process measured by the BESIII and Belle Collaborations recently, we evaluate this process at $\mathcal{O}(\alpha_s^4)$ accuracy in the framework of nonrelativistic QCD. We find that the cross section at the center-of-mass energy $\sqrt{s} = 4.009$ GeV is 34.6pb, which is consistent with the BESIII data. The comparison with the Belle data in the region from 4.0 GeV to 5.3 GeV is also presented. Concerning the η and η' mixing and the potential gluonium component of η' , we also estimate the rate of $e^+e^- \rightarrow \eta' J/\psi$ process, which can be checked within the updated Belle data.

PACS numbers: 12.38.Bx, 13.66.Bc, 14.40.-n

I. INTRODUCTION

The quarkonium spectroscopy has represented a unique inspection window on strong interaction for more than thirty years, and keeps on attracting great interests from both theorists and experimentalists up to now. It is well-known that the Constituent Quark Model (CQM) predicts perfectly the spectroscopy of charmonium in the scope below $D\bar{D}$ threshold, but still has to rise to the challenge in the region above the threshold [1]. In this region, a plethora of new states confirmed by different experiments are in or beyond the spectroscopy anticipated by the CQM. On one hand, conventional resonances such as $\psi(3770)$, $\psi(4040)$, $\psi(4160)$, and $\psi(4415)$, whose quantum numbers can be predicted by CQM, strongly couple to open charm final states and then have broad widths[2]. On the other hand, many newly observed charmonium-like states with $J^{PC} = 1^{--}$, the Y(4260), Y(4360), and Y(4660), exhibit an exotic nature, which couple to hidden charm final states with large partial widths [3]. This suggests that these states may have different structures with respect to their conventional descriptions within the CQM.

By studying the hadronic transition to a lower charmonium state like J/ψ and a light meson like η , we can investigate the properties of those conventional or unconventional states in question. The CLEO collaboration measured the cross section of $e^+e^- \rightarrow \eta J/\psi$ as $15^{+5}_{-4} \pm 8$ pb at $\sqrt{s} = 4.12 - 4.20$ GeV eight years ago [4]. Recently, the BESIII Collaboration has measured the cross section of $e^+e^- \rightarrow \eta J/\psi$ at $\sqrt{s} = 4.009$ GeV [5]. The result is $\sigma(e^+e^- \rightarrow \eta J/\psi)(\sqrt{s} = 4.009 \text{ GeV}) =$

$(32.1 \pm 2.8 \pm 1.3)$ pb, which is a large value. And the Belle Collaboration has also measured the cross section of the same channel by scanning the center-of-mass energy from 3.8 GeV to 5.3 GeV [6]. They show us that the cross sections are around 70 pb and 50 pb when the center-of-mass energy are near the $\psi(4040)$ and $\psi(4160)$ peaks respectively. We can imagine that the resonance effects play an important role in those energy areas. The pioneering work studying the open charm effects in this process can be found in Ref. [7]. Therein the cross section of $e^+e^- \rightarrow \eta J/\psi$ is calculated via virtual D meson loops at \sqrt{s} from 3.7 GeV to 4.3 GeV. And, in those regions, the results are in agreement with the experimental data with suitable choices of input parameters.

In this paper, we adopt the nonrelativistic QCD (NRQCD) scheme and calculate the cross section of $e^+e^- \rightarrow \eta J/\psi$ at \sqrt{s} from 4.0 GeV to 5.3 GeV. It is known that higher-order corrections to the expansion in the strong coupling constant α_s can solve the discrepancy problem in double charmonium production at the B-factory [8–11]. In this paper the cross section of $e^+e^- \rightarrow \eta^{(\prime)} J/\psi$ is investigated at order of $\mathcal{O}(\alpha_s^4)$. Our aim is to understand whether the data can be explained at order $\mathcal{O}(\alpha_s^4)$.

Hereafter, η and η' are treated with the Light-Cone (LC) approach while J/ψ is treated with NRQCD. The η and η' mixing effect is also important, as has been widely discussed in, e.g. in Refs. [12–16], and will be taken into account in our considerations. η can be described on either flavor octet-singlet or quark-flavor basis, however for η' the gluonium content may have a role in the interaction. According to the conservation of parity and charge conjugation, the leading-order in α_s expansion for $e^+e^- \rightarrow \eta^{(\prime)} J/\psi$ comes from the diagrams where two gluons transit to $\eta^{(\prime)}$. In this case, the color-singlet Fock state of J/ψ dominates the contribution.

This paper is organized as follows: after the Introduc-

*Electronic address: qiaocf@ucas.ac.cn

†Electronic address: zhuruilin09@mails.ucas.ac.cn

tion, the Sec. II contains the formulae used in our analysis. Therein we introduce the LC distribution amplitude for each component of the $\eta^{(\prime)}$ meson. The effective $\eta^{(\prime)}gg$ vertex is employed within the LC approach. Our numerical results for the cross section are given in Sec. III, where the comparison with the BESIII and Belle data are also presented. The last section is reserved to conclusions.

II. PRODUCTION MECHANISM

In the literature, two schemes exist to describe the η and η' mixing [17]:

- with respect to the flavor octet and singlet bases, where the basis vectors are $\eta_8 = (u\bar{u} + d\bar{d} - 2s\bar{s})/\sqrt{6}$ and $\eta_0 = (u\bar{u} + d\bar{d} + s\bar{s})/\sqrt{3}$. Then the states can be decomposed as

$$\begin{pmatrix} |\eta\rangle \\ |\eta'\rangle \end{pmatrix} = \begin{pmatrix} \cos\theta & -\sin\theta \\ \sin\theta & \cos\theta \end{pmatrix} \begin{pmatrix} |\eta_8\rangle \\ |\eta_0\rangle \end{pmatrix}; \quad (1)$$

- with respect to the quark-flavor (QF) bases, where the basis vectors are $\eta_q = (u\bar{u} + d\bar{d})/\sqrt{2}$ and $\eta_s = s\bar{s}$, then

$$\begin{pmatrix} |\eta\rangle \\ |\eta'\rangle \end{pmatrix} = \begin{pmatrix} \cos\phi & -\sin\phi \\ \sin\phi & \cos\phi \end{pmatrix} \begin{pmatrix} |\eta_q\rangle \\ |\eta_s\rangle \end{pmatrix}. \quad (2)$$

In what follows, we perform our calculation using the QF bases, and the latest value of the mixing angle measured by the KLOE Collaboration is $(41.5 \pm 0.3 \pm 0.7 \pm 0.6)^\circ$ [18]. Using the definition in (2), we can get the corresponding decompositions for η and η'

$$|\eta\rangle = \cos\phi |\eta_q\rangle - \sin\phi |\eta_s\rangle, \quad (3)$$

$$|\eta'\rangle = \sin\phi |\eta_q\rangle + \cos\phi |\eta_s\rangle. \quad (4)$$

In the above decomposition, we still do not consider the gluonium component, which, however, can be important in η' [19]. Hence we should take the gluonium component

into account in the analysis for η' . On the other hand, the QCD sum rules has told us that the gluonium couples to η much more weakly than to η' [19]. In this case we will adopt the traditional view and ignore the gluonium component in the η meson. Based on this argument, an additional mixing angle ϕ_G is introduced, and the gluonium component is defined as $|\eta_g\rangle = |gg\rangle$, then the η' state is reparametrized as

$$|\eta'\rangle = \cos\phi_G(\sin\phi |\eta_q\rangle + \cos\phi |\eta_s\rangle) + \sin\phi_G |\eta_g\rangle. \quad (5)$$

Next we turn to the LC distribution amplitudes of those components. The LC distribution amplitude of the η_q or η_s component in η can be expanded in Gegenbauer polynomials [17]

$$\Phi(x, \mu) = 6x\bar{x}(1 + \sum_{n=1}^{\infty} B_{2n}(\mu) C_{2n}^{3/2}(x - \bar{x})), \quad (6)$$

where x and $\bar{x} = 1 - x$ are the momentum fractions of the two partons inside the $\eta_{q,s}$ component respectively. The scale dependence of $B_n(\mu)$ at leading-order logarithmic accuracy can be written as

$$B_n(\mu) = \left(\frac{\alpha_s(\mu)}{\alpha_s(\mu_0)} \right)^{\frac{\gamma_n}{\beta_0}} B_n(\mu_0), \quad (7)$$

where the anomalous dimension reads as

$$\gamma_n = 4C_F(\psi(n+2) + \gamma_E - \frac{3}{4} - \frac{1}{2(n+1)(n+2)}), \quad (8)$$

being $\psi(n)$ the digamma function. Here μ_0 is the typical hadronic energy scale below which non-perturbative evolution takes place. And all those contributions are summed up into the factor $B_n(\mu_0)$. In the following calculation, $B_2(1\text{GeV}) = 0.2$ is adopted, which is determined from QCD Sum Rules [20].

For the η' state, the mixing effect between quark and gluonium components should be taken into account. Then we take the following form for the LC distribution amplitudes [21]

$$\begin{aligned} \Phi^{(q,s)}(x, \mu) &= 6x\bar{x} \left\{ 1 + \left[B_2^{(q,s)}(\mu_0) \left(\frac{\alpha_s(\mu^2)}{\alpha_s(\mu_0^2)} \right)^{\frac{48}{81}} - \frac{B_2^{(g)}(\mu_0)}{90} \left(\frac{\alpha_s(\mu^2)}{\alpha_s(\mu_0^2)} \right)^{\frac{101}{81}} \right] C_2^{3/2}(x - \bar{x}) + \dots \right\}, \\ \Phi^{(g)}(x, \mu) &= x\bar{x}(x - \bar{x}) \left[16B_2^{(q,s)}(\mu_0) \left(\frac{\alpha_s(\mu^2)}{\alpha_s(\mu_0^2)} \right)^{\frac{48}{81}} + 5B_2^{(g)}(\mu_0) \left(\frac{\alpha_s(\mu^2)}{\alpha_s(\mu_0^2)} \right)^{\frac{101}{81}} \right] + \dots \end{aligned} \quad (9)$$

According to the NRQCD scheme[22, 23], the physical state J/ψ is expanded in the Fock space according to powers of v , the relative velocity of the heavy quark in

the quarkonium. The expansion can be written as

$$|J/\psi\rangle = \mathcal{O}(1)|c\bar{c}[^3S_1^{(1)}]\rangle + \mathcal{O}(v)|c\bar{c}[^3P_J^{(8)}]g\rangle + \mathcal{O}(v^2). \quad (10)$$

Then let us consider the quark-level diagrams for the process $e^+e^- \rightarrow \eta^{(\prime)} J/\psi$, which are depicted in Figs. 1 and 2. With regard to the conservation of parity and charge conjugation, the leading-order contribution in α_s expansion comes from Fig. 1 where the light meson $\eta^{(\prime)}$ is emitted in the transition from two gluons. The color-singlet Fock state dominates the hadronization of J/ψ while the contribution from color-octet Fock state has a suppression factor of order $v^2 \alpha_s$. In Fig. 2, the relevant diagrams for two gluons transiting to different components of $\eta^{(\prime)}$ are depicted.

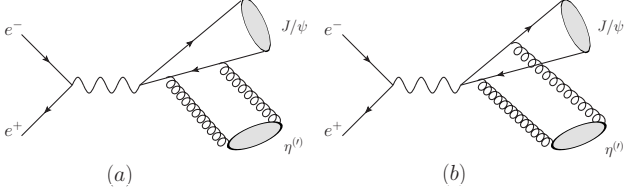


FIG. 1: The typical Feynman diagrams for electron-positron to $\eta^{(\prime)} J/\psi$ transition.

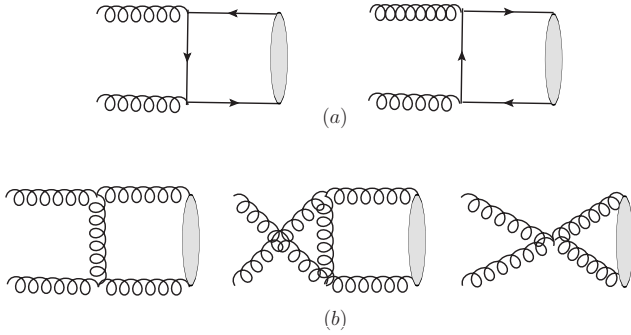


FIG. 2: The Feynman diagrams for two gluons transiting to different components of $\eta^{(\prime)}$: (a) to the meson's quark component and (b) to its gluonium component.

The effective $\eta^{(\prime)} g^* g^*$ vertex from the meson's quark component, as shown in Fig. 2(a), can be constructed as

$$\mathcal{M}^{(q)} \equiv -i F_{\eta^{(\prime)} g^* g^*}^{(q)}(q_1^2, q_2^2, m_{\eta^{(\prime)}}^2) \delta_{ab} \varepsilon^{\mu\nu\rho\sigma} \varepsilon_\mu^{a*} \varepsilon_\nu^{b*} q_{1\rho} q_{2\sigma}, \quad (11)$$

where q_1 and q_2 are the momenta of two virtual gluons respectively. $F_{\eta^{(\prime)} g^* g^*}^{(q)}$ represents the transition form factor, and its expression is

$$F_{\eta^{(\prime)} g^* g^*}^{(q)}(q_1^2, q_2^2, m_{\eta^{(\prime)}}^2) = \frac{2\pi\alpha_s(\mu^2)}{N_c} \sum_{a=q,s} f_{\eta^{(\prime)}}^a \int_0^1 dx \times \Phi^{(a)}(x, \mu) \left[\frac{1}{xq_1^2 + \bar{x}q_2^2 - x\bar{x}m_{\eta^{(\prime)}}^2 + i\epsilon} + (x \leftrightarrow \bar{x}) \right], \quad (12)$$

here, the momentum exchange invariance between q_1 and q_2 obviously holds. The factors $f_{\eta^{(\prime)}}^a$ are relevant to the

decay constants of $|\eta_q\rangle$ and $|\eta_s\rangle$ [24]

$$f_\eta^q = f_q \cos \phi, \quad f_\eta^s = -f_s \sin \phi, \quad (13)$$

$$f_{\eta'}^q = f_q \sin \phi, \quad f_{\eta'}^s = f_s \cos \phi. \quad (14)$$

We adopt the value of the decay constants of η_q and η_s from Ref. [17]

$$f_q = (1.07 \pm 0.02)f_\pi, \quad f_s = (1.34 \pm 0.06)f_\pi,$$

with the pion's decay constant 0.130 GeV [25].

Furthermore, the effective $\eta' g^* g^*$ vertex can be defined as

$$\mathcal{M}^{(g)} \equiv -i F_{\eta' g^* g^*}^{(g)} \delta_{ab} \varepsilon^{\mu\nu\rho\sigma} \varepsilon_\mu^{a*} \varepsilon_\nu^{b*} q_{1\rho} q_{2\sigma}, \quad (15)$$

where the transition form factors $F_{\eta' g^* g^*}^{(g)}$ have been calculated in Ref.[21]

$$F_{\eta' g^* g^*}^{(g)}(q_1^2, q_2^2, m_{\eta'}^2) = \frac{4\pi\alpha_s(\mu^2)}{Q^2} \frac{C}{2} \int_0^1 dx \Phi^{(g)}(x, \mu) \times \left[\frac{xq_1^2 + \bar{x}q_2^2 - (1+x\bar{x})m_{\eta'}^2}{\bar{x}q_1^2 + xq_2^2 - x\bar{x}m_{\eta'}^2 + i\epsilon} - (x \leftrightarrow \bar{x}) \right], \quad (16)$$

where $C = \sqrt{2} f_q \sin \phi + f_s \cos \phi$, and $Q^2 = |q_1^2 + q_2^2|$. Note that the LC distribution amplitude of the gluonium component is asymmetrical when we exchange the momentum fractions x and \bar{x} in equation (9). Given the consideration, it can be seen that the form factor in equation (16) is actually invariant by exchange of the momenta of the incoming gluons.

Following the notation above, the amplitude of $e^+e^- \rightarrow \eta J/\psi$ at order $\mathcal{O}(\alpha_s^4)$ can be obtained. The result is presented in APPENDIX A. To manipulate the trace and matrix element square, the Mathematica software is employed with the help of the packages FeynCalc[26], FeynArts[27], and LoopTools[28]. The amplitudes are Ultra-Violet and Infra-Red safe, and they can be calculated in four dimensions.

III. PRODUCTION CROSS SECTION

In this section, we calculate the cross section of $e^+e^- \rightarrow \eta^{(\prime)} J/\psi$. To compare with the experimental data measured by the BESIII and Belle collaborations, we vary the center-of-mass energy from 4 GeV to 5.3 GeV. In the numerical calculation, the following values of input parameters are adopted [29]

$$m_{J/\psi} = 3.096 \text{ GeV}, \quad m_\eta = 547.8 \text{ MeV}, \quad m_{\eta'} = 957.7 \text{ MeV},$$

$$m_c = 1.40 \text{ GeV}, \quad \alpha = 1/127, \quad \Gamma_{ee}^{J/\psi} = 5.55 \text{ keV}.$$

The radial wave function squared at the origin of the J/ψ is extracted from its leptonic width at leading-order of α_s [30], i.e.,

$$|R(0)|_{J/\psi}^2 = \frac{m_{J/\psi}^2 \Gamma(J/\psi \rightarrow e^+e^-)}{4\alpha^2 e_c^2}. \quad (17)$$

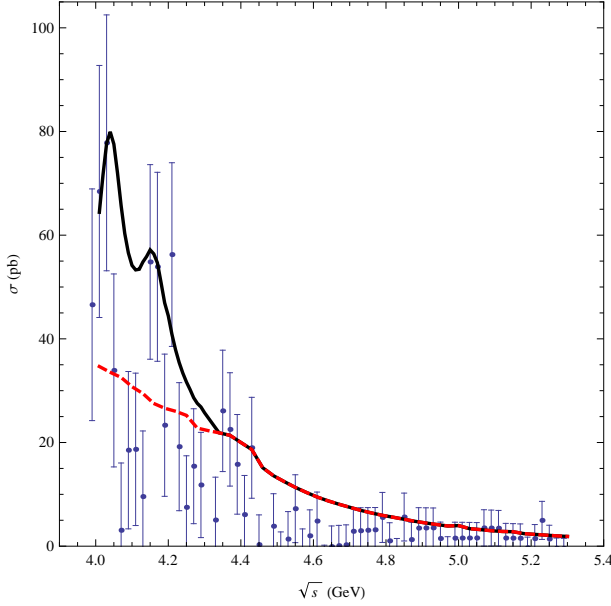


FIG. 3: The cross section of $e^+e^- \rightarrow \eta J/\psi$ versus center-of-mass energy \sqrt{s} . The dashed line is the cross section including the contributions shown in Fig. 1, while the solid line is the result after considering the resonance state effects, for which we adopt the effective coupling constants $g_{\psi(X)c\bar{c}} g_{\psi(X)e^+e^-} = \sqrt{5}e^2/100$. And the data is measured by the Belle collaboration [6].

Then the J/Ψ 's Schrödinger wave function squared at the origin can be obtained from $|\psi(0)|_{J/\Psi}^2 = |R(0)|_{J/\Psi}^2/4\pi$, with numerical value of 0.0446 GeV^3 .

Thus the cross section for the process $e^+e^- \rightarrow \eta J/\psi$ can be obtained. At center-of-mass energy $\sqrt{s} = 4.009 \text{ GeV}$, the numerical result is 34.6 pb . The result is consistent with the measurement $32.1 \pm 2.8 \pm 1.3 \text{ pb}$ obtained by the BESIII Collaboration. We can conclude that the two-gluons transition dominates the creation of η and higher order contribution should be suppressed by a small K factor.

For the comparison with the data measured by the Belle Collaboration at \sqrt{s} from 4 GeV to 5.3 GeV, the production mechanism presented in Figs. 1 and 2 is in-

complete in specific energy regions. In fact, we should take into account the resonance-state effects or the open-charm effects when \sqrt{s} is near the resonance states which are strongly coupling to $\eta J/\psi$. In the regions when \sqrt{s} is near the $\psi(4040)$ and $\psi(4160)$ peaks, the virtual D-meson loop effect becomes important[7, 31–33]. Here, we adopt the effective coupling constants $g_{\psi(X)c\bar{c}}$ and $g_{\psi(X)e^+e^-}$ with $X = 4040, 4160$ to phenomenologically describe the resonance effects. We can write the resonance $\psi(X)$ transition amplitude as

$$M = \bar{v}_{e^-} \gamma^\alpha u_{e^+} \frac{g_{\psi(X)c\bar{c}} g_{\psi(X)e^+e^-} (-g^{\alpha\beta} + \frac{p^\alpha p^\beta}{m_{\psi(X)}^2})}{e(s - m_{\psi(X)}^2 + im_{\psi(X)}\Gamma_{\psi(X)})} M_\beta, \quad (18)$$

where p denotes the momentum of the virtual photon in Fig. 1, e is related to the electromagnetic coupling constant with $e^2 = 4\pi\alpha$, $m_{\psi(X)}$ and $\Gamma_{\psi(X)}$ represent the mass and the decay width of $\psi(X)$ respectively, while M_β can be obtained through a virtual photon emitted to $\eta J/\psi$ at order $\mathcal{O}(\alpha_s^4)$.

We plot our results and experimental data together in Fig. 3. There the \sqrt{s} dependence of the cross section of $e^+e^- \rightarrow \eta J/\psi$ is presented. The dashed line is the contribution from Fig. 1, while the solid line is the contribution after considering the resonance state effects. We find that the cross section at the $\psi(4040)$ and $\psi(4160)$ peaks can be well explained when we fix the effective coupling constants $g_{\psi(X)c\bar{c}} g_{\psi(X)e^+e^-} = \sqrt{5}e^2/100$.

In comparison with the result based on open charm effect in Ref. [7], we find that our results are consistent with those when the phase parameters are chosen as $(\theta, \beta, \phi) = (0, 0, 0)$.

Finally, to allow the experimental search for a signal of gluonium component in η' we have calculated the cross sections with and without such contribution. The results are given in Table I. There we assume, as in Ref. [34], that 26% of gluonic admixture exists in η' , i.e. $\sin^2\phi_G^2 = 0.26$. The numerical results show that such contribution from the gluonium component can affect the total cross section by up to a 17.0% variation. This possibility can be checked in the upcoming Belle experiment. We also find that the cross section decreases rapidly with increasing scattering energy.

TABLE I: The cross sections (in pb) of $e^+e^- \rightarrow \eta' J/\psi$ at different center-of-mass energies \sqrt{s} . Here σ_w and $\sigma_{w/o}$ represent the cross sections with and without the gluonium component contribution respectively.

$\sqrt{s}(\text{GeV})$	4.3	4.4	4.5	4.6	4.7	4.8	4.9	5.0	5.1	5.2	5.3
$\sigma_{w/o}$	41.2	29.2	19.7	14.5	11.1	8.84	6.78	5.37	4.29	3.46	2.79
σ_w	34.1	24.2	16.4	12.6	9.9	8.23	6.51	5.22	4.24	3.45	2.82
$\frac{ \sigma_w - \sigma_{w/o} }{\sigma_{w/o}}$	17.0%	16.8%	16.3%	13.4%	10.0%	6.9%	3.9%	2.7%	1.3%	0.2%	1.1%

IV. CONCLUSIONS

Motivated by the large cross section of $e^+e^- \rightarrow \eta J/\psi$ process observed by the BESIII and Belle Collaborations, we have evaluated this process in the framework of NRQCD. We find that the cross section at $\sqrt{s} = 4.009$ GeV is 34.6pb, which is in agreement with the BESIII data when its uncertainty is taken into account. And our results can also explain the energy dependence measured by the Belle Collaboration. Inspired by this calculation, we have also estimated the cross section for $e^+e^- \rightarrow \eta' J/\psi$ process, where the contribution of two gluons transiting to η' is treated within the LC approach.

The electronic production of $\eta^{(\prime)} J/\psi$ has a crucial phenomenological significance. Color-singlet transitions dominate the formation of the accompanying J/ψ and color-octet Fock states are suppressed by a factor of $v^2\alpha_s$. This clear hadronization structure of J/ψ allows us to focus on the interesting mixing effect between η and η' and differentiate the quark and gluonium components of the η' . Concerning the η , the comparison between the experimental data for $e^+e^- \rightarrow \eta J/\psi$ and our calculations confirm the traditional view that the probability of a gluonium component in η is negligible.

The cross section dependence on the center-of-mass energy \sqrt{s} for $e^+e^- \rightarrow \eta J/\psi$ will provide a platform to investigate the properties of resonance states such as $\psi(4040)$ and $\psi(4160)$. By measuring the cross section and comparing it with the contribution from Fig. 1, one can also hunt the signals for the potential resonances strongly coupling to $\eta J/\psi$ and(or) measure their branching ratios.

Finally, we have taken the gluonium component into account for $e^+e^- \rightarrow \eta' J/\psi$. The gluonium component has been investigated in many processes where a heavy meson decays to η' and a light meson. Here we have studied it in electroproduction. In the energy scan region of the Belle experiment, we calculated the contributions from both quark and gluonium components. Numerical results show that the gluonium component contributions would decrease the total cross section by up to 17%, an effect that can be detected in the upcoming experiment.

Acknowledgements:

R. Z. thanks Prof. Feng Yuan for useful discussions. This work was supported in part by the National Natural Science Foundation of China(NSFC) under the grants 10935012, 11121092, 11175249, and 11375200.

Appendix A: Amplitude of $e^+e^- \rightarrow \eta J/\psi$

In this appendix, the amplitude of $e^+e^- \rightarrow \eta J/\psi$ is given at $\mathcal{O}(\alpha_s^4)$ accuracy in the framework of nonrelativistic QCD. In the formula below, s is the center-of-mass energy squared, x and \bar{x} are the momentum-fractions of the two partons inside the η meson component, $\Phi(x)$ is the light-cone distribution amplitude of η_q , ε is the polarization vector of J/ψ , and B_0 , C_0 , and D_0 are scalar Passarino-Veltman integrals defined in Ref. [28]. Besides, we indicate the amplitudes of the processes (a) and (b) in Fig. 1 with \mathcal{M}_a and \mathcal{M}_b , respectively. The total amplitude can be written as $\mathcal{M} = 2\mathcal{M}_a + 2\mathcal{M}_b$.

$$\begin{aligned}
\mathcal{M}_a = & \int_0^1 dx \frac{32\sqrt{6}\pi\sqrt{m_c}\epsilon_{\lambda\mu\nu\rho}\varepsilon^\mu p_c^\nu p_q^\rho \bar{v}_e\gamma^\lambda u_e \Phi(x)\psi(0)_{J/\psi} C_F \alpha_s^2}{9s(-8m_c^2(m_\eta^2 + s) + 16m_c^4 + (s - m_\eta^2)^2)} \sum_{a=u,d,s} f_\eta^a \times \left\{ \frac{m_\eta^4(-4m_c^2 + m_\eta^2 - s)}{-4m_c^2 + m_\eta^2 + s} D_1 \right. \\
& - \frac{(m_c^2((16 - x(4x + 11))m_\eta^2 + s(16 - 13x)) + 4(7x - 8)m_c^4 + (x - 1)(3sxm_\eta^2 + (x + 2)m_\eta^4 + 2s^2))}{(x - 1)(-4m_c^2 + m_\eta^2 + s)} C_1 \\
& + \frac{(4m_c^2 - m_\eta^2 + s)(x(x + 1)m_\eta^2 - m_c^2)}{x(-4m_c^2 + m_\eta^2 + s)} C_2 + 2m_\eta^2 C_3 + \frac{(-4m_c^2 + m_\eta^2 + 3s)B_0(\frac{1}{2}(-2m_c^2 + m_\eta^2 + s), 0, m_c^2)}{(x - 1)(-4m_c^2 + m_\eta^2 + s)} \\
& - \frac{x(-4m_c^2 + m_\eta^2 + 3s)B_0((1 - 2x)m_c^2 + \frac{1}{2}x((2x - 1)m_\eta^2 + s), 0, 0)}{(x - 1)(-4m_c^2 + m_\eta^2 + s)} + 2B_0((x - 1)^2m_\eta^2, 0, 0) \\
& + \frac{(-4(x - 1)m_c^2 + (x - 1)m_\eta^2 + 3sx + s)B_0((1 - 2x)m_c^2 + \frac{1}{2}x((2x - 1)m_\eta^2 + s), 0, m_c^2)}{x(-4m_c^2 + m_\eta^2 + s)} \\
& + \frac{B_0(m_c^2, 0, 0)(-4m_c^2 + m_\eta^2 - s)}{x(-4m_c^2 + m_\eta^2 + s)} - 2B_0(x^2m_\eta^2, 0, 0) + (x \leftrightarrow \bar{x}) \Big\}, \tag{A1}
\end{aligned}$$

$$\begin{aligned}
\mathcal{M}_b = & - \int_0^1 dx \frac{32\sqrt{6}\pi\sqrt{m_c}\epsilon_{\lambda\mu\nu\rho}\varepsilon^\mu p_c^\nu p_q^\rho \bar{v}_e \gamma^\lambda u_e \Phi(x)\psi(0)_{J/\Psi} C_F \alpha_s^2}{9sx^2(16m_c^4 - 8(m_\eta^2 + s)m_c^2 + (s - m_\eta^2)^2)} \sum_{a=u,d,s} f_\eta^a \times \left\{ \frac{4x(4m_c^2 + 2m_\eta^2 - s)m_c^2}{x-1} D_2 \right. \\
& + \frac{4xm_\eta^2(4m_c^2 + (2x^2 + 2x + 1)m_\eta^2 - s)m_c^2}{4m_c^2 + m_\eta^2 - s} D_3 + 4xm_\eta^2 C_3 - \frac{4(4(3x-2)m_c^2 + (3-2x)xm_\eta^2 + s(2-3x))m_c^2}{(x-1)(4m_c^2 + m_\eta^2 - s)} C_4 \\
& - \frac{4(x-1)(-4m_c^2 + (2x+1)m_\eta^2 + s)m_c^2}{4m_c^2 + m_\eta^2 - s} C_5 + \frac{2x(16m_c^4 - 8(s-2xm_\eta^2)m_c^2 + (4x^3-1)m_\eta^4 + s^2 - 4sxm_\eta^2)m_c^2}{(x-1)(-4m_c^2 - m_\eta^2 + s)} D_4 \\
& + \frac{4(-4(x-1)m_c^4 + ((2x^2+3x-1)m_\eta^2 + s(x-1))m_c^2 + xm_\eta^2(m_\eta^2 - s))}{-4m_c^2 - m_\eta^2 + s} C_1 - \frac{2x(4m_c^2 + (2x-1)m_\eta^2 - s)}{x-1} C_7 \\
& - \frac{2(-8(2x^2-5x+2)m_c^4 + 2(x(4x^2-1)m_\eta^2 + s(2x^2-7x+2))m_c^2 + x(s-m_\eta^2)((1-2x)m_\eta^2 + s))}{(x-1)(-4m_c^2 - m_\eta^2 + s)} C_8 \\
& + \frac{2x(-4m_c^2 - m_\eta^2 + s)}{x-1} C_6 + \frac{2(16(3x-1)m_c^4 + 4((-2x^2+4x+1)m_\eta^2 + s-4sx)m_c^2 + x(s-m_\eta^2)^2)}{(x-1)(4m_c^2 + m_\eta^2 - s)} C_9 \\
& - \frac{x(-32m_c^6 + 16(m_\eta^2 + 2s)m_c^4 - 2(3m_\eta^4 + 4s(x-1)m_\eta^2 + 5s^2)m_c^2 + (s-m_\eta^2)^2((2x-1)m_\eta^2 + s))}{-4m_c^2 - m_\eta^2 + s} D_5 \\
& + \frac{2xm_\eta^2((8-16x)m_c^4 + 2((2x^2-2x+1)m_\eta^2 + s(4x-1))m_c^2 - x(s-m_\eta^2)^2)}{4m_c^2 + m_\eta^2 - s} D_6 + (x \leftrightarrow \bar{x}) \Big\}, \tag{A2}
\end{aligned}$$

where

$$\begin{aligned}
D_1 &= D_0(m_c^2, m_\eta^2, f_1, f_3, x^2 m_\eta^2, 0, 0, m_c^2, 0), \\
D_2 &= D_0(m_c^2, f_3, m_c^2, f_3, s, m_\eta^2, 0, 0, m_c^2, m_c^2), \\
D_3 &= D_0(m_c^2, x^2 m_\eta^2, \bar{x}^2 m_\eta^2, f_3, f_1, m_\eta^2, 0, 0, 0, m_c^2), \\
D_4 &= D_0(m_c^2, x^2 m_\eta^2, f_2, s, f_1, f_3, 0, 0, 0, m_c^2, m_c^2), \\
D_5 &= D_0(f_1, f_2, m_c^2, f_3, s, \bar{x}^2 m_\eta^2, 0, 0, m_c^2, m_c^2), \\
D_6 &= D_0(x^2 m_\eta^2, f_3, m_c^2, \bar{x}^2 m_\eta^2, f_2, m_\eta^2, 0, 0, 0, m_c^2), \\
C_1 &= C_0(f_3, \bar{x}^2 m_\eta^2, f_1, 0, m_c^2, 0), \\
C_2 &= C_0(m_c^2, x^2 m_\eta^2, f_1, 0, 0, m_c^2), C_9 = C_2|_{x \rightarrow 1}, \\
C_3 &= C_0(m_\eta^2, x^2 m_\eta^2, \bar{x}^2 m_\eta^2, 0, 0, 0), \\
C_4 &= C_0(m_c^2, s, f_3, m_c^2, 0, m_c^2), \\
C_5 &= C_0(m_c^2, \bar{x}^2 m_\eta^2, f_2, 0, 0, m_c^2), \\
C_6 &= C_0(m_c^2, s, f_3, 0, m_c^2, m_c^2), \\
C_7 &= C_0(f_3, x^2 m_\eta^2, f_2, m_c^2, 0, 0), \\
C_8 &= C_0(s, f_2, f_1, 0, m_c^2, m_c^2), \\
f_1 &= (\bar{x} - x)m_c^2 + \frac{1}{2}x((x - \bar{x})m_\eta^2 + s), \\
f_2 &= \frac{1}{2}(2(x - \bar{x})m_c^2 - \bar{x}((\bar{x} - x)m_\eta^2 + s)), \\
f_3 &= \frac{1}{2}(-2m_c^2 + m_\eta^2 + s). \tag{A3}
\end{aligned}$$

- lision (2012), Strbske Pleso, Slovakia, arXiv:1212.2169.
- [3] B. Aubert et al. (BABAR Collaboration), Phys. Rev. Lett. **95**, 142001 (2005); C. Z. Yuan et al. (Belle Collaboration), Phys. Rev. Lett. **99**, 182004 (2007); X. -L. Wang et al. (Belle Collaboration), Phys. Rev. Lett. **99**, 142002 (2007).
 - [4] T. E. Coan *et al.* (CLEO Collaboration), Phys. Rev. Lett. **96**, 162003 (2006).
 - [5] M. Ablikim et al. (BESIII Collaboration), Phys. Rev. D **86**, 071101 (2012).
 - [6] X. -L. Wang et al. (Belle Collaboration), Phys. Rev. D **87**, 051101 (2013).
 - [7] Q. Wang, X. -H. Liu, and Q. Zhao, Phys. Rev. D **84**, 014007 (2011).
 - [8] B. Aubert et al. (BABAR Collaboration), Phys. Rev. D **72**, 031101 (2005) ; K. Abe et al. (Belle Collaboration), Phys. Rev. D **70**, 071102 (2004).
 - [9] K. -Y. Liu, Z. -G. He, and K. -T. Chao, Phys. Lett. B **557**, 45(2003); E. Braaten and J. Lee, Phys. Rev. D **67**, 054007 (2003); K. Hagiwara, E. Kou, and C. -F. Qiao, Phys. Lett. B **570**, 39 (2003).
 - [10] Y. -J. Zhang, Y. -J. Gao, and K. -T. Chao, Phys. Rev. Lett. **96**, 092001 (2006); B. Gong and J. -X. Wang, Phys. Rev. D **77**, 054028 (2008).
 - [11] Z. -G. He, Y. Fan, and K. -T. Chao, Phys. Rev. D **75**, 074011 (2007).
 - [12] A. Bramon, R. Escribano, and M. D. Scadron, Eur. Phys. J. C **7**, 271 (1999).
 - [13] G. Ricciardi, Phys. Rev. D **86**, 117505 (2012); C. D. Donato, G. Ricciardi, and I. Bigi, Phys. Rev. D **85**, 013016 (2012).
 - [14] Y. -Y. Fan, W. -F. Wang, S. Cheng, and Z. -J. Xiao, Phys. Rev. D **87**, 094003 (2013); X. Liu, H. -N. Li, and Z. -J. Xiao, Phys. Rev. D **86**, 011501 (2012).
 - [15] S. Dubnicka, A. Z. Dubnickova, M. A. Ivanov, and A. Lip-taj, Phys. Rev. D **87**, 074201 (2013).
 - [16] A. I. Ahmadov, D. G. Kostunin, and M. K. Volkov, Phys. Rev. C **87**, 045203 (2013).
 - [17] T. Feldmann, P. Kroll, and B. Stech, Phys. Rev. D **58**, 114006 (1998); T. Feldmann, Int. J. Mod. Phys. A **15**, 159 (2000).
 - [18] F. Ambrosino et al. (KLOE Collaboration), Phys. Lett. B **648**, 267 (2007).
 - [19] F. D. Fazio and M. R. Pennington, J. High Energy Phys. **07** (2000) 051.
 - [20] P. Ball, J. High Energy Phys. **01** (1999) 010.
 - [21] A. Ali and A. Y. Parkhomenko, Phys. Rev. D **65**, 074020 (2002); T. Muta and M. -Z. Yang, Phys. Rev. D **61**, 054007 (2000).
 - [22] G. T. Bodwin, E. Braaten, and G. P. Lepage, Phys. Rev. D **51**, 1125 (1995).
 - [23] C. -F. Qiao, L. -P. Sun, and P. Sun, J. Phys. G **37**, 075019 (2010); C. -F. Qiao, L. -P. Sun, and R. -L. Zhu, J. High Energy Phys. **08** (2011) 131.
 - [24] K. Azizi, R. Khosravi, and F. Falahati, Phys. Rev. D **82**, 116001 (2010).
 - [25] C. -F. Qiao, P. Sun, D. Yang, and R. -L. Zhu, Phys. Rev. D **89**, 034008 (2014).
 - [26] R. Mertig, M. Bohm, and A. Denner, Comput. Phys. Commun. **4**, 345 (1991).
 - [27] T. Hahn, Comput. Phys. Commun. **140**, 418 (2001).
 - [28] T. Hahn and M. Perez-Victoria, Comput. Phys. Commun. **118**, 153 (1999).
 - [29] J. Beringer et al. (Particle Data Group), Phys. Rev. D **86**, 010001 (2012).
 - [30] C. -F. Qiao and R. -L. Zhu, Phys. Rev. D **87**, 014009 (2013).
 - [31] Z. -G. Guo, S. Narison, J. -M. Richard, and Q. Zhao, Phys. Rev. D **85**, 114007 (2012); G. Li, X. -H. Liu, Q. Wang, and Q. Zhao, Phys. Rev. D **88**, 014010 (2013); Q. Wang, C. Hanhart, and Q. Zhao, Phys. Rev. Lett. **111**, 132003 (2013).
 - [32] D. -Y. Chen, X. Liu, and T. Matsuki, Phys. Rev. D **87**, 054006 (2013).
 - [33] F. -K. Guo, C. Hanhart, and U. -G. Meissner, Phys. Rev. Lett. **103**, 082003 (2009); **104**, 109901E (2010).
 - [34] E. Kou and A. I. Sanda, Phys. Lett. B **525**, 240 (2002).